SOL ENGINEERING SERVICES

Test Infrastructure, Validation, and Quality Assurance for AM Thermal Hardware

Flow loops, heater blocks and single-jet rigs, proof and leak testing, micro-CT inspection, through-thickness conductivity measurement, validation of surrogate predictions against hardware and university test capacity in Alabama and Mississippi

Prepared for DEVCOM Army Research Laboratory, the Ground Vehicle Systems Center, and university and industry partners of the CF-JET effort

Classification	Unclassified. Prepared from open-source information.
Date	26 November 2026

Executive Summary

Instruments alone can verify the thermal resistance of a cold plate at 0.02 K/W to about ±3.0 percent at 1.5 kW (computed, Table 2), yet published rig studies show that the definition of case temperature and the joining pressure shift the same quantity by 3.3 to 42.9 percent.[12] The test definition therefore governs the answer more than the thermocouples do. A written test definition, a measurement of the interface and a guard-banded acceptance limit decide whether a hardware result can confirm or reject a surrogate prediction. This paper examines the standards, the through-thickness conductivity methods, the inspection by micro-computed tomography and the statistics of comparing prediction intervals with measurements, and it reports what Alabama and Mississippi laboratories document.

- **Standards cover procedure and omit accuracy.** The Open Compute Project cold plate specification defines resistance as (Ts − Tl) / P, requires six or more flow rates between 25 and 150 percent of rated flow for pressure drop, and lists helium, pressure-decay, hydrostatic and burst tests. It states no sample size and no numeric measurement uncertainty.[3] Its reference fluid temperature of 45 °C differs from the 65 °C inlet of the CF-JET design point (Table 1).
- **The test definition outweighs the instruments.** Instrument terms give ±3.0 percent on resistance (computed, Table 2). One university rig reported an uncertainty of ±10.6 percent at 0.0198 K/W, a 42.9 percent gap between averaged and extrapolated case temperature, and 34.2 percent higher resistance at 10 psi than at 15 psi.[4] A measured value of 0.0195 K/W has a 31.9 percent chance of exceeding 0.02 K/W at the university rig's uncertainty and 4.8 percent at the instrument-only level (computed, Table 3).
- **Heat-balance checks need a matched temperature pair.** Coolant rise at 1.5 kW is 6.4 K at 4 L/min and 3.2 K at 8 L/min (computed), so thermocouple limits of ±0.5 K give 13 to 25 percent on the calorimetric power (Table 4).
- **No standard fits a thin anisotropic composite.** ASTM E1461 states its scope as primarily homogeneous isotropic solids, and ASTM D5470 reports apparent conductivity for heterogeneous materials.[5][6] A computed Monte Carlo of a five-thickness D5470 regression recovered conductivity within about ±22 percent at 100 W/m·K, while a single 1 mm specimen read 50 W/m·K because of contact resistance (Table 7). No retrieved source reports measured through-thickness conductivity for pitch-fiber-insert composites.
- **Micro-CT resolves features at three to six voxels.** A KU Leuven study reports rapidly growing error for defects under three times the voxel size, and a simulation study sets six voxels across a void for porosity errors under 10 percent.[7][8] A 60 mm plate scanned in one view with a 2,000-pixel detector has a voxel of about 30 µm (computed), which leaves features under 90 µm undetected (Table 9).
- **Intervals need noise-aware comparison and enough points.** When measurement noise equals the prediction deviation, a 95 percent interval covers 83 percent of measured values (computed, Table 10). Distinguishing 95 percent from 85 percent coverage needs 46 validation points (computed, Figure 5).
- **Documented university capacity covers printing and manufacturing training.** Auburn documents an X-ray CT system, Calhoun, Mississippi Gulf Coast and East Mississippi document additive manufacturing labs, and Alabama A&M, Tuskegee and Jackson State document printing and materials equipment. No retrieved source documents a flow loop, laser flash or thermal cycling at an HBCU or community college in either state (Table 12).

1. Introduction and Scope

The CF-JET proposal replaces a conventional jet-impingement cold plate with a three-dimensional printed body that has interleaved return ports and a carbon fiber target plate with perpendicular pitch fiber inserts, sealed by a thin electroplated coolant face. The design point is 1.5 kW on a 60 mm by 60 mm footprint with 50/50 water-glycol entering at 65 °C at 4 to 8 L/min, a pressure drop of 30 kPa or less and a thermal resistance of 0.02 K/W, which implies an average heat flux of 41.7 W/cm² and a 30 K rise from coolant to case at full load (derived).[9] The effort responds to ARL-BAA-0107 and draws on ARL-BAA-0038 and elements of ARL-BAA-0064.

Figure 1. Test and validation ladder for CF-JET thermal hardware

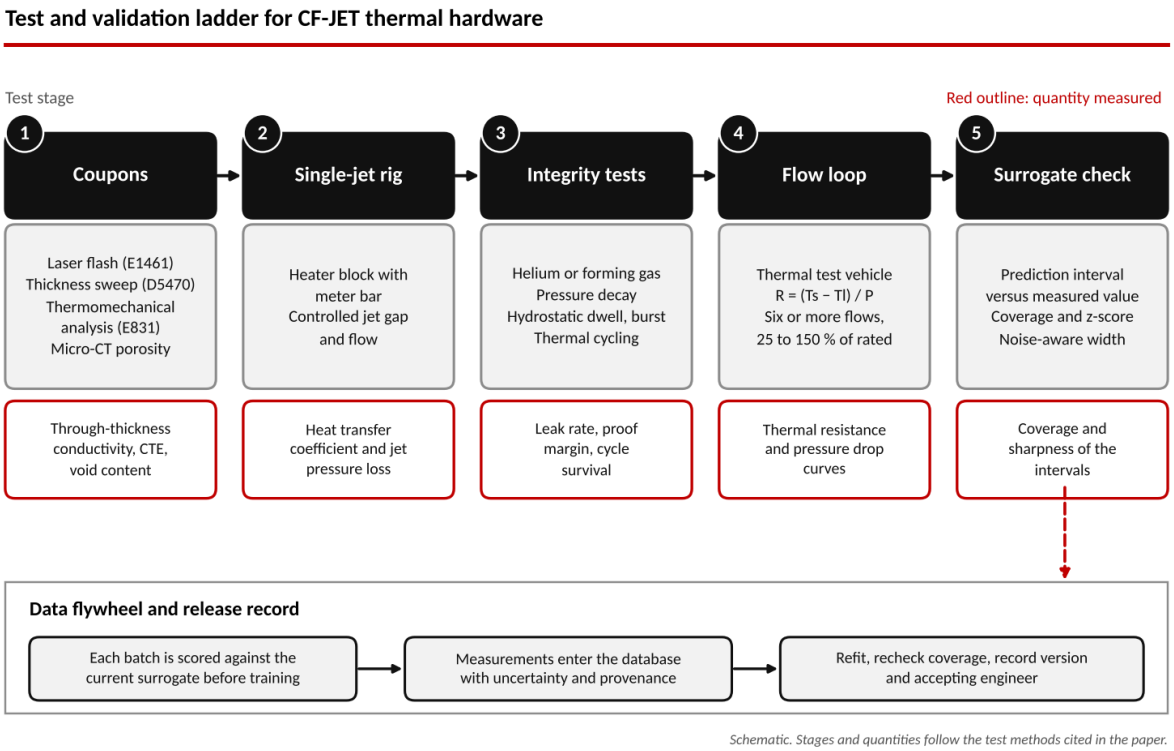

Stages follow the test methods cited in this paper. The diagram is schematic and shows no measured data.

SOL Engineering Services describes a software pipeline, SOL Aquifer, that codifies engineering steps as code: scripted condition sweeps, physics solvers in code, a SQL database that records provenance, and surrogate training with uncertainty quantification.[10] The same documents describe uncertainty-aware neuro-symbolic inference and a data flywheel that recalibrates from coupon, single-jet and prototype data. SOL Aquifer originated in HVAC modeling work done with Alabama A&M University students.[11] Every prediction of such a surrogate is a claim about hardware, and hardware tests supply the evidence that confirms or rejects it.

Figure 1 shows the ladder of tests that this paper examines. Coupons give material properties, a single-jet rig gives local heat transfer, integrity tests establish that a part holds pressure, a flow loop gives the thermal resistance and pressure drop of the assembled plate, and a comparison of prediction intervals with those measurements validates the surrogate. Each stage produces numbers with an uncertainty that the downstream stages inherit. The scope covers flow loops, heater blocks, single-jet rigs, proof and leak testing, thermal cycling fixtures, micro-computed tomography, measurement of through-thickness

conductivity and thermal expansion, validation of surrogate predictions, and the university laboratories in Alabama and Mississippi that could support the work.

Five questions organize the review. Which test methods and standards apply to cold plate thermal resistance, pressure drop and leak integrity? Which methods measure through-thickness conductivity in thin anisotropic composites, and with what uncertainty? What does micro-CT detect in additively manufactured polymer and composite parts, and at what resolution? How should prediction intervals be compared with measured results? Which university capabilities in Alabama and Mississippi support this work? Where the literature supplies numbers, the paper reports them with their source. Where it does not, a calculation computed for this paper supplies a quantity, and its inputs are stated in the table notes.

2. Cold Plate Thermal Resistance, Pressure Drop and Leak Integrity

2.1 The published specification defines the procedure and leaves accuracy to each laboratory

The Open Compute Project published a single-phase direct-to-chip cold plate test specification, version 1.0.0, dated 11 August 2026.[12] Its primary author and one co-author are affiliated with a cold plate manufacturer, and the other co-authors are affiliated with PFX Group, Fabric8Labs and INFICON. The specification defines thermal resistance as (Ts − Tl) / P, where Ts is the temperature at the base of the cold plate, Tl is the incoming fluid temperature and P is the applied power, measured on a thermal test vehicle with the recommended interface material. The procedure bleeds the loop, stabilizes flow, applies power, records temperature, pressure drop, power and flow at steady state, and repeats at several flow rates to build a performance curve.

Pressure drop is measured at constant flow with inlet and outlet pressures, and the specification subtracts a tare reading taken with the loop and without the cold plate. It requires at least six flow rates from 25 to 150 percent of rated flow, including 100 percent, tests bidirectional plates in both directions, and reports a curve fit with coefficients A and B. Leak and proof testing has four parts: helium or forming-gas detection with a dwell of 5 to 10 minutes and an example criterion under 0.6 SCCM for water-tight, gas pressure decay with a dwell of 5 to 30 minutes and an example criterion under 0.5 percent loss, a hydrostatic dwell at maximum rated operating pressure for 5 minutes and at three times that pressure for 2 minutes, and a destructive burst test with a rise rate of 1 to 5 bar/min after ISO 18869.[13] Table 1 lists the methods with the conditions that the specification gives.

Table 1. Test methods for cold plate resistance, pressure drop and leak integrity

Test	Procedure	Conditions and acceptance example	Evidence
Thermal resistance	R = (Ts − Tl) / P on a thermal test vehicle with the recommended interface material; bleed loop, stabilize, record	Fluid at 45 °C ± 2 °C; meets the product specification at every tested flow rate	Industry specification[14]
Pressure drop	Inlet and outlet pressure at constant flow; subtract tare reading with the loop alone	At least six flows from 25 to 150 percent of rated flow; curve-fit coefficients A and B; both directions for bidirectional plates	Industry specification[15]
Helium or forming-gas leak	Sealed part pressurized with 5 % hydrogen in nitrogen or helium; vacuum chamber, sniffer probe or immersion	Dwell 5 to 10 minutes; example criterion under 0.6 SCCM for water-tight	Industry specification[16]
Gas pressure decay	Air or nitrogen; observe pressure over the dwell	Dwell 5 to 30 minutes; example criterion under 0.5 percent loss	Industry specification[17]

Test	Procedure	Conditions and acceptance example	Evidence
Hydrostatic dwell	Liquid-filled; maximum rated operating pressure, then three times that pressure; dimensions before and after	5 minutes then 2 minutes at 20 to 25 °C; no detectable leak or deformation	Industry specification[18]
Burst	Destructive; pressure rises until rupture or three times minimum proof pressure	Rise rate 1 to 5 bar/min after ISO 18869; example criterion over 20 bar	Industry specification[19]
Flow range	Increase flow to a velocity under 1.5 m/s and check for erosion or leaks	Fluid at 25 °C ± 5 °C	Industry specification[20]
Metrology rig for resistance	Standard thermal test vehicle with a heat-flux-meter bar; case temperature extrapolated with Fourier's law	1000 W, 1 to 4 L/min, inlet 22 to 42 °C, 25 vol % propylene glycol	Peer-reviewed rig study[21]

The specification gives example criteria and states that each test should define its own resolution and uncertainty. It states no sample sizes and no numeric measurement accuracy.

Three gaps separate the specification from the CF-JET design point. The reference fluid temperature of 45 °C is 20 K under the 65 °C inlet of the design point, so resistance tests of CF-JET hardware need a custom set point whose effect on viscosity and conductivity is recorded. The rated-flow range of 4 to 8 L/min implies tested flows from 1 to 12 L/min under the 25 to 150 percent rule (derived). The pressure limit of 30 kPa makes a 1 percent resolution equal to 0.3 kPa (derived), which sets the transducer and tare requirements. The specification contains no numeric accuracy, and the retrieved literature contains no standards-body document for a resistance metrology method at the 0.02 K/W level. The nearest document is a university proposal for a thermal metrology standard.[22]

2.2 Case-temperature definition and joining pressure change measured resistance more than the instruments do

The Villanova University group built a standard thermal test vehicle for cold plates: a copper block with four 750 W cartridge heaters and a 50 mm by 50 mm by 50 mm heat-flux-meter bar with four Type K thermocouples, a flow loop with 25 percent propylene glycol, and uncertainty propagation by the Moffat root-sum-square method.[23] Validation of the vehicle gave a resistance of 0.0198 ± 0.0021 K/W, which is ±10.6 percent.[24] The group compared three definitions of case temperature: the center thermocouple, the average of three surface thermocouples, and a temperature extrapolated from the meter bar with Fourier's law, which the authors treat as the true value. The average and the extrapolated value gave resistances that differed by 42.9 percent with a shallow coolant groove and by 9.0 percent with a deeper groove, and the center and average values differed by 3.3 percent.[25] Resistance at 10 psi joining pressure was 34.2 percent higher than at 15 psi with grease, and a phase-change pad (PTM) gave 36.6 percent lower resistance than grease.[26]

These findings bear on CF-JET in two ways. The 0.02 K/W target is close to the 0.0198 K/W of the validation, so the reported ±10.6 percent applies at the same magnitude. The CF-JET stack also differs from a copper block, since the heat enters a carbon fiber target plate through an interface that the test vehicle must reproduce. A resistance quoted without the interface material, the joining pressure and the case-temperature definition cannot be compared with a surrogate prediction. The acceptance statement for the design point needs to name all three, and the surrogate needs the same quantities as inputs.

The instrument terms are small by comparison. Table 2 computes them for the design point from stated limits: Type T thermocouples with a special limit of ±0.5 °C, which governs because 0.4 percent of 95 °C is 0.38 K,[27] a heater power meter at ±0.5 percent and a heat loss of ±1 percent of power. Each limit is treated as a rectangular distribution, and the combined standard uncertainty is expanded with k = 2. The result is

±3.0 percent, or ±0.0006 K/W, and the two thermocouples supply 82 percent of the combined variance. The 30 K case-to-inlet rise at full load is what keeps the temperature terms small, and the same terms would reach 27 percent of resistance at a 3 K rise (derived).

Table 2. Instrument uncertainty budget for thermal resistance at 1.5 kW (computed)

Term	Assumed limit	Expanded contribution to R, k = 2	Evidence for the input
Case thermocouple	±0.5 K, Type T special limit	1.9 %	Vendor tolerance table[28]
Inlet thermocouple	±0.5 K, Type T special limit	1.9 %	Vendor tolerance table[29]
Heater power meter	±0.5 % of power	0.6 %	Assumed
Heat loss to surroundings	±1 % of power	1.2 %	Assumed
Combined	Root-sum-square of rectangular terms	3.0 % (±0.0006 K/W)	Computed

Computed from R = (Tc − Tin) / Q with Q = 1500 W and R = 0.02 K/W, so the case-to-inlet rise is 30 K. Each limit is divided by the square root of 3 and the combined value is doubled. The power meter and heat-loss limits are assumed values.

Figure 2. Instrument terms compared with published rig effects on thermal resistance

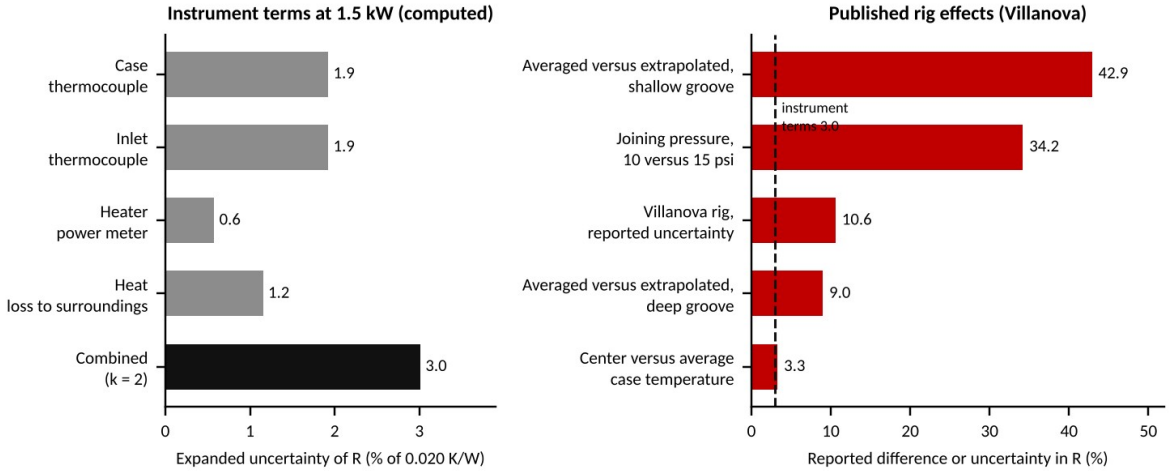

The left panel is computed from Table 2. The right panel reports differences and uncertainty from the Villanova studies and applies to their cold plate and rig.[30][31]

2.3 A guard-banded acceptance limit protects against accepting resistance that exceeds the requirement

A requirement of 0.02 K/W or lower has an acceptance risk when the measured value lies near the limit. A simple guard band lowers the acceptance limit by the expanded uncertainty. With instrument terms alone the limit becomes 0.0194 K/W, and with the ±10.6 percent of the university rig it becomes 0.0179 K/W (computed). Table 3 shows the probability that true resistance exceeds 0.02 K/W given a measured value, for a normal measurement error with the standard uncertainty of each case and a flat prior. A reading of 0.0195 K/W has a 4.8 percent chance of exceeding the limit at the instrument-only level and 31.9 percent at the level of the university rig. The value of the exercise is the difference between the two columns: the uncertainty claimed for the rig decides how close to the limit a plate can be accepted.

Table 3. Probability that true resistance exceeds 0.02 K/W given a measured value (computed)

Measured resistance (K/W)	Instrument terms only, ±3.0 % (k = 2)	University rig level, ±10.6 % (reported)
0.0180	0.0 %	3.0 %
0.0190	0.0 %	17.3 %
0.0195	4.8 %	31.9 %
0.0200	50.0 %	50.0 %

Computed with a normal error whose standard deviation is half the expanded value and a flat prior on true resistance. The instrument-only column uses Table 2. The second column applies the reported ±0.0021 K/W on 0.0198 K/W to a rig that may differ from CF-JET.

2.4 Calorimetric power checks lose accuracy at design flow unless the temperature pair is matched

A heat balance on the coolant gives an independent check on heater power, and it is the usual control for heat loss. The coolant rise at 1.5 kW is 6.4 K at 4 L/min, 4.3 K at 6 L/min and 3.2 K at 8 L/min, using a density of 1015 kg/m^3 and a specific heat of 3450 J/(kg·K) for 50/50 water-glycol (assumed property values). Thermocouples with ±0.5 K limits give 13 percent uncertainty on the calorimetric power at 4 L/min and 25 percent at 8 L/min (Table 4), which is far looser than the ±0.5 percent power meter. A matched inlet and outlet pair with a 0.05 K limit, an assumed value, gives 1.3 to 2.5 percent. A Bell Labs thermal-interface apparatus reports thermistor measurements to ±0.001 K, so matched pairs at this level exist in research apparatus.[32] The calorimetric check is useful at CF-JET flows only with such a pair, and the heater power meter remains the primary power measurement.

Table 4. Calorimetric heat-balance uncertainty at 1.5 kW (computed)

Flow (L/min)	Coolant rise (K)	Thermocouples, ±0.5 K limits (% of power, k = 2)	Matched pair, ±0.05 K limit (% of power, k = 2)
4	6.4	12.7	1.3
6	4.3	19.1	1.9
8	3.2	25.4	2.5

Computed from Q = 1500 W, density 1015 kg/m^3 and specific heat 3450 J/(kg·K), which are assumed values for 50/50 water-glycol near 65 °C. Temperature terms only; flow-meter uncertainty is excluded. The 0.05 K limit is assumed.

2.5 Pressure-decay criteria depend on internal volume, and a 1 K gas drift consumes most of a 0.5 percent limit

The specification gives a pressure-decay example of under 0.5 percent loss over the dwell and a helium example of under 0.6 SCCM.[33] The two criteria are linked by the internal volume and the dwell. For a loss of 0.5 percent of an absolute pressure of 300 kPa, a leak rate follows from the volume divided by the dwell time (computed). Table 5 shows that a 50 mL internal volume with a 5 minute dwell corresponds to 0.15 SCCM, and a 20 mL volume with a 30 minute dwell corresponds to 0.01 SCCM. The pressure-decay criterion resolves leaks well under the 0.6 SCCM helium example at these volumes.

Temperature drift limits the resolution in practice. A 1 K change in gas temperature changes absolute pressure by 1.02 kPa at 300 kPa, which is 68 percent of the 0.5 percent criterion of 1.5 kPa (computed with the ideal gas law at constant volume). A decay test on a part that has just been handled, filled or cycled needs a thermal soak and a temperature record to separate leakage from drift. A helium test measures gas leaving the part and does not depend on a pressure change, so gas temperature affects it less (derived).

Table 5. Leak rate equivalent to a 0.5 percent pressure loss at 300 kPa absolute (computed)

Internal volume (mL)	5 minute dwell (SCCM)	10 minute dwell (SCCM)	30 minute dwell (SCCM)
20	0.06	0.03	0.01
50	0.15	0.07	0.02
100	0.30	0.15	0.05

Computed as 0.005 × 300 kPa × volume ÷ dwell, converted with 1 SCCM = 1.689 × 10^{-3} Pa·m^3/s. The pressure and volumes are assumed values; the 0.5 percent and 0.6 SCCM criteria are examples from the specification.

3. Through-Thickness Conductivity and Thermal Expansion

3.1 Neither laser flash nor D5470 states scope for a thin anisotropic composite with oriented inserts

ASTM E1461 determines thermal diffusivity by the flash method, with a stated range of 0.1 to 1000 mm^2/s, and its catalog scope describes primarily homogeneous isotropic solid materials.[34] Conductivity follows from diffusivity, specific heat and density, so its uncertainty combines three measurements. An older edition of the standard states that the method strictly applies to homogeneous solids and advises caution for porous or heterogeneous specimens, a statement that bears on carbon fiber with pitch inserts.[35] A carbon fiber plate with perpendicular pitch fiber inserts is inhomogeneous at the scale of the insert pitch, and its through-thickness behavior differs from its in-plane behavior by design.

ASTM D5470 measures steady-state thermal impedance and calculates an apparent thermal conductivity for materials from liquids to hard solids. The standard calls the result apparent because the materials are usually heterogeneous, and it imposes an idealized heat-flow pattern.[36] A thickness sweep separates contact resistance from bulk resistance: the slope of impedance against thickness gives the reciprocal of conductivity and the intercept gives the contact term. A Bell Labs apparatus built on the D5470 meter-bar approach reports thermistor temperature measurement to ±0.001 K,[37] and a University of Arkansas modification with three thermocouples per side and an interface material reduced reported measurement uncertainty by 42.85 percent for titanium and 48.81 percent for pyrolytic graphite.[38] The thesis attributes the effect to contact resistance, which matters more for higher-conductivity materials.

Table 6. Methods for through-thickness conductivity of thin composites

Method	Quantity measured	Stated scope or limit	Uncertainty evidence	Evidence
Laser flash, ASTM E1461	Through-thickness thermal diffusivity; conductivity needs specific heat and density	Primarily homogeneous isotropic solids; 0.1 to 1000 mm^2/s	None retrieved for pitch-fiber-insert composites; propagation in Table 8 (computed)	Standard catalog[39]
Steady-state meter bar, ASTM D5470	Thermal impedance; apparent conductivity	Heterogeneous materials allowed; idealized one-dimensional heat flow	Contact resistance dominates at high conductivity; thickness sweep separates it	Standard catalog[40]
Modified D5470 with interface material	Out-of-plane conductivity of graphite and titanium	Three thermocouples per side; regression on thickness	Uncertainty cut by 42.85 percent (titanium) and 48.81 percent (graphite)	Honors thesis[41]
High-precision meter-bar apparatus	Thermal impedance of interface materials	Thermistors at ±0.001 K; simultaneous electrical resistance	Corporate laboratory summary	Corporate record[42]

No retrieved source reports through-thickness conductivity of a composite with perpendicular pitch fiber inserts at 50 to 300 W/m·K, the range that the CF-JET concept implies.

3.2 Contact resistance biases a single-specimen reading low by 33 to 75 percent at 50 to 300 W/m·K

A Monte Carlo calculation for this paper shows how contact resistance acts on a D5470-type measurement of a 1 mm specimen. The inputs are assumed: a contact resistance of 10 mm²·K/W summed over both interfaces with 20 percent specimen-to-specimen variation, thickness errors of 5 µm and measurement noise of 2 percent. At a true conductivity of 50 W/m·K the bulk resistance of a 1 mm specimen is 20.0 mm²·K/W, and a single reading gives 33 W/m·K. At 100 W/m·K the reading is 50 W/m·K, and at 300 W/m·K it is 75 W/m·K, since the contact term of 10 mm²·K/W exceeds the bulk term of 3.3 mm²·K/W (Table 7, Figure 3). A single-thickness reading therefore reports a lower bound.

A regression on five thicknesses from 0.5 to 3 mm recovers the conductivity with a median of 50, 100 and 299 W/m·K at the three true values, and the 95 percent range widens from 45 to 57 W/m·K at 50 W/m·K to 185 to 764 W/m·K at 300 W/m·K. The regression is unbiased in this model and its precision falls as conductivity rises, because the bulk term of a thin specimen shrinks toward the scatter of the contact term. The result gives a requirement for the CF-JET coupons: several thicknesses, a controlled interface material and a record of contact pressure. It also shows that a quoted conductivity over 100 W/m·K from a single specimen deserves a contact-resistance estimate before it enters a surrogate. The calculation is a model with assumed inputs, and no composite was measured.

Table 7. Estimated conductivity from a D5470-type measurement with contact resistance (computed)

True conductivity (W/m·K)	Bulk resistance, 1 mm (mm²·K/W)	Single 1 mm specimen, median (95 % range) (W/m·K)	Five-thickness regression, median (95 % range) (W/m·K)
50	20.0	33 (29 to 39)	50 (45 to 57)
100	10.0	50 (42 to 62)	100 (82 to 127)
300	3.3	75 (58 to 107)	299 (185 to 764)

Monte Carlo with 20,000 trials. Contact resistance 10 mm²·K/W summed over two interfaces with 20 % variation, thickness error 5 µm, resistance noise 2 %, thicknesses 0.5, 1.0, 1.5, 2.0 and 3.0 mm. All inputs are assumed.

Figure 3. Contact-resistance bias in a D5470-type measurement and laser flash timing

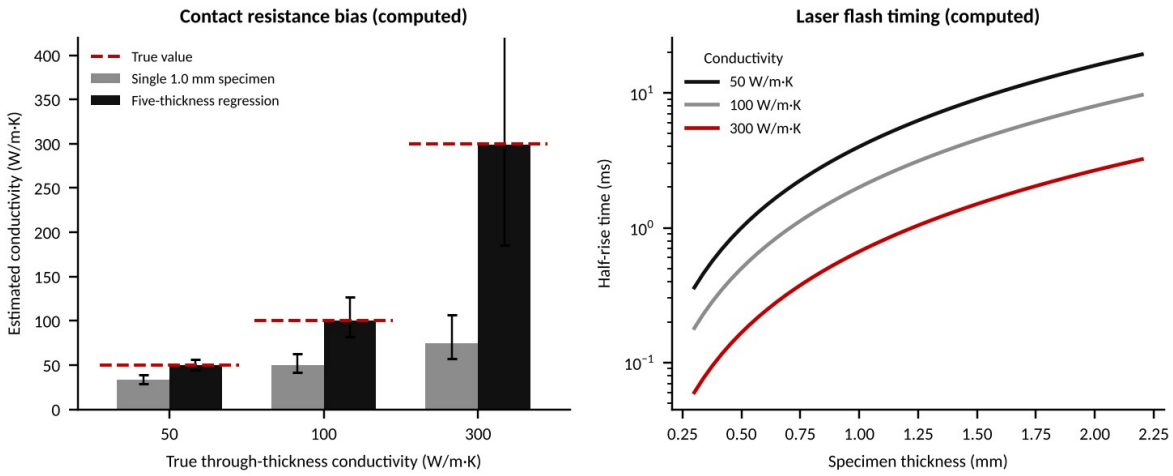

Both panels are computed with assumed inputs listed in Table 7 and Table 8. The left panel shows the median and 95 percent range of the estimate.

3.3 Laser flash timing for a 1 mm plate falls between 0.7 and 4 ms, and conductivity inherits

three uncertainties

The half-rise time of a flash measurement follows $t_{½} = 0.1388\ L^2 / \alpha$, where L is the specimen thickness and α is the diffusivity. For an assumed density of 1800 kg/m³ and specific heat of 800 J/(kg·K), conductivities of 50 to 300 W/m·K give diffusivities of 35 to 208 mm²/s, inside the 0.1 to 1000 mm²/s range of the standard. Table 8 shows half-rise times of 0.67 to 4.00 ms for a 1 mm plate and 0.17 to 1.00 ms for a 0.5 mm plate. Times of this order require a record of the instrument pulse width and detector response, because a pulse that lasts a sizeable fraction of the half-rise time biases the result. No retrieved source gives the pulse width of a specific instrument, and none is assumed here.

Conductivity is the product of diffusivity, density and specific heat. For assumed relative standard uncertainties of 5 percent on diffusivity, 1 percent on density and 3 percent on specific heat, plus thickness error of 10 µm that enters twice because diffusivity scales with L^2, the combined relative standard uncertainty on conductivity is 6.2 percent for a 1 mm plate and 7.1 percent for a 0.5 mm plate (computed, Table 8). These values apply to a homogeneous specimen. For a plate with inserts the specimen diameter must cover several insert pitches for the one-dimensional model to hold, and a lateral diffusion check with a thermal camera or a segmented detector would test the assumption. No retrieved source reports such a check on a pitch-fiber composite.

Table 8. Laser flash half-rise time and conductivity uncertainty for a thin plate (computed)

Thickness (mm)	Half-rise time at 50 W/m·K (ms)	Half-rise time at 100 W/m·K (ms)	Half-rise time at 300 W/m·K (ms)	Relative standard uncertainty of conductivity (%)
0.5	1.00	0.50	0.17	7.1
1.0	4.00	2.00	0.67	6.2
2.0	15.99	7.99	2.66	6.0

Computed with $t_{½} = 0.1388\ L^2 / \alpha$, density 1800 kg/m³ and specific heat 800 J/(kg·K). The uncertainty combines assumed values of 5 % on diffusivity, 1 % on density, 3 % on specific heat and 10 µm on thickness.

3.4 Thermomechanical analysis loses accuracy for plates designed under 5 µm/(m·°C)

ASTM E831 determines the coefficient of linear thermal expansion by thermomechanical analysis and recommends a lower limit of 5 µm/(m·°C), with decreased accuracy and precision at lower or negative values.[43] A carbon fiber plate designed for low in-plane expansion falls under that limit. A 10 mm specimen heated through 100 K expands by 1 µm at 1 µm/(m·°C), 2 µm at 2, 4 µm at 4 and 5 µm at 5 (derived), so the signal is a few micrometers and the probe, specimen and fixture expansion are of the same size. The correction for the fixture, a calibration with a reference material of similar expansion and an uncertainty statement belong in the test plan. The standard offers no accuracy value for the low range in the retrieved catalog text, and the retrieved sources contain no measurement of near-zero expansion composites on this apparatus. Thermal cycling of the assembled plate follows JEDEC JESD22-A104 for temperature cycling, which defines the cycle conditions that a fixture must reproduce.[44]

4. Micro-CT Inspection of Additively Manufactured Polymer and Composite Parts

4.1 Micro-CT detects voids, bundle defects and print-path faults, and detection requires at least three voxels across a feature

A KU Leuven study scanned 3D-printed carbon fiber reinforced polyamide at a 6 µm isotropic voxel and identified seven classes of defect: channel pores between beads in pure polyamide layers, pores along the outer shell of the concentric fiber pattern, voids within and between fiber bundles, large voids where the fiber path ends early, voids where the fiber path starts and the polyamide wall layers are interrupted, voids in the corners between bundles and walls, and twisting or buckling of bundles.[45] The overall porosity of the scanned part averaged 6.7 percent, with 5 to 12 percent across individual slices, and the full fiber section reached 9.7 percent. The authors state that error rises rapidly for defects under three times the voxel size and that smaller voids are absent from the scans. At 6 µm that threshold is about 18 µm.[46]

A simulation study by Plank, Sause and Kastner generated synthetic carbon fiber composite scans with known porosity and derived a voxel-size rule from the ratio of void surface area to volume. The minimum voxel size is one sixth of the equivalent void diameter, which assumes at least six voxels across the object and aims at an error under 10 percent.[47] For a specimen with 2.25 volume percent porosity the rule gave a minimum voxel of about 6.3 µm, and global thresholding errors were −5.7 percent at 5 µm and −30.2 percent at 10 µm. With thresholds adapted to each specimen, the mean error in overall porosity across six specimens was 1.95 percent at 2.5 µm, 4.65 percent at 5 µm and 16.58 percent at 10 µm. The study notes that a change of matrix material or scan setup requires recalibration of the threshold, and that it excludes phase-contrast effects that can make micro-voids more visible in real scans.[48] A benchmarking study from Oak Ridge reports that micro-CT detects finer pores than image analysis of sections yet limits the sample volume and underestimates porosity because of spatial variation.[49]

4.2 A single-view scan of a 60 mm plate has a voxel near 30 µm, and finer voxels multiply the number of scans

Voxel size follows from the field of view divided by the detector pixel count, so a larger part costs resolution. For an assumed detector width of 2,000 pixels, a 60 mm plate in one view gives a 30 µm voxel, which detects features of 90 µm and quantifies features of 180 µm at the three-voxel and six-voxel rules (computed, Table 9, Figure 4). A 5 µm voxel detects 15 µm features and quantifies 30 µm features, and it limits the field of view to 10 mm, so a 60 mm by 60 mm area needs 36 tiles in one plane. Cone-beam geometry and the plate thickness change these figures, and the table treats the field of view as the specimen width at the detector.

Table 9. Micro-CT feature limits and scan coverage for a 60 mm by 60 mm plate (computed)

Voxel size (µm)	Detectable at 3 voxels (µm)	Quantifiable at 6 voxels (µm)	Field of view (mm)	Tiles to cover the plate
2.5	7.5	15	5	144
5	15	30	10	36
10	30	60	20	9
25	75	150	50	4
30	90	180	60	1

Computed for an assumed 2,000-pixel detector width, so field of view equals 2,000 times the voxel size. The three-voxel limit follows the KU Leuven statement and the six-voxel limit follows the Plank rule.[5051] *The calculation ignores cone-beam geometry and plate thickness.*

Figure 4. Micro-CT feature limits and scan tiles against voxel size

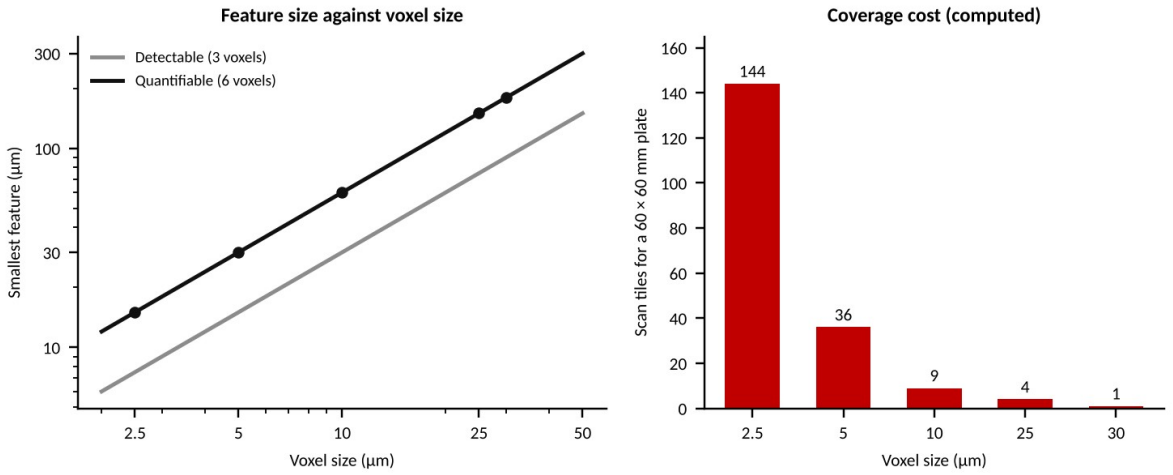

Both panels are computed from Table 9 under the stated assumptions.

Three consequences follow for the CF-JET plate. Full-plate inspection at 30 µm detects voids and bundle faults of 90 µm and larger, which includes macroscopic voids. Characterization of pore populations that affect conductivity needs voxels of 5 µm or finer on coupons or sub-regions, and the thresholds need calibration against a section or a known-porosity specimen. The thin electroplated coolant face and its bond to the body are the least documented feature: no retrieved study reports micro-CT of an electroplated polymer or composite cold plate, so the detectability of plating voids and delamination is a gap that a trial scan of a representative coupon would close. Auburn University documents an X-ray CT system for additive manufacturing parts acquired with a 2016 NIST grant, and it is the only CT facility found in the two states.[52]

5. Validation of Surrogate Predictions Against Hardware

5.1 A prediction interval covers a measured value only after the measurement noise is added to its width

A surrogate reports a distribution for the true response, and a test reports the true response plus measurement noise. Comparing an interval built for the true response with a noisy measurement lowers the observed coverage. For a prediction deviation σp and a measurement deviation σm, the observed coverage of a nominal 95 percent interval is $2\Phi(1.96 / \sqrt{(1 + r^2)}) - 1$ with $r = \sigma m / \sigma p$ (computed). Coverage falls to 92.0 percent at r = 0.5 and 83.4 percent at r = 1 (Table 10, Figure 5). A multi-fidelity Gaussian process study forms the interval for noisy outputs by replacing the predictive deviation with the root of its square plus the noise variance.[53] ASME V&V 20 frames the same point for simulation: the comparison error between simulation and data is judged against a validation uncertainty that includes experimental data uncertainty.[54]

The adjustment has a practical consequence for CF-JET. The resistance rig of Table 2 has a relative standard uncertainty of 1.5 percent by its instruments and 5.3 percent at the level of the university rig. If the surrogate predicts resistance with a standard deviation of 5 percent, the university-level noise gives r near 1 and the surrogate appears miscalibrated when it is not. Each hardware batch then needs the measurement uncertainty from Table 2 and Table 8, entered as σm, before coverage is scored. Replicates at identical settings estimate σm directly.

Table 10. **Observed coverage of a nominal 95 percent interval when measurement noise is ignored (computed)**

Noise ÷ prediction deviation, r	Theoretical coverage (%)	Observed in a set of 20 points, mean (sd) (%)	Width factor that restores 95 %
0.0	95.0	95.1 (4.9)	1.00
0.5	92.0	92.1 (5.9)	1.12
1.0	83.4	83.4 (8.5)	1.41

Computed for normal prediction error and normal measurement noise, with 4,000 simulated validation sets of 20 points. The width factor is $\sqrt{(1 + r^2)}$.

Figure 5. **Interval coverage against measurement noise and exact intervals on observed coverage**

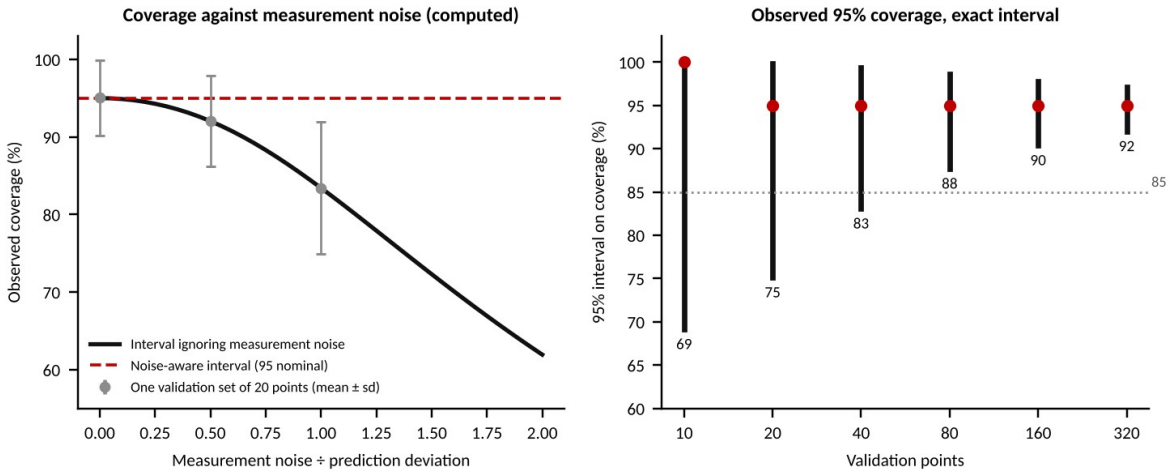

Left panel computed from the formula in the text with simulated sets of 20 points. Right panel computed with Clopper-Pearson intervals for 95 percent observed coverage.

5.2 Distinguishing 95 percent coverage from 85 percent needs about 46 validation points

Observed coverage from a few points has a wide uncertainty. An exact binomial interval for 19 covered points of 20 spans 75 to 100 percent, and for 38 of 40 it spans 83 to 99 percent (computed, Figure 5). The lower bound reaches 85 percent at 46 points and 90 percent at 127 points when observed coverage is 95 percent. A validation set that is wrong, with true coverage of 85 percent, shows an upper bound under 95 percent in 19 percent of sets of 10 points, 36 percent of sets of 20, 56 percent of sets of 40 and 87 percent of sets of 80 (computed). A prototype program that produces a few dozen measured plates cannot certify 95 percent coverage in one region, and a statement of coverage needs the count behind it.

Conformal methods give a finite-sample guarantee on marginal coverage, and a small calibration set spreads the realized coverage widely around that average, often under the target.[5556] A study of neural surrogates for engineering simulation reports interval coverage and the root mean square of standardized residuals as calibration checks, with targets of 0.95 and 1, and it shows validation-based rescaling moving coverage toward nominal.[57] Dataset shift lowers calibration for several model types, which makes coverage a property of a region of the input space and of a hardware batch.[58] Table 11 lists the metrics that the validation plan can use.

Table 11. **Calibration metrics for comparing prediction intervals with measurements**

Metric	What it checks	Target	Limit	Evidence
Interval coverage	Fraction of measured values inside the prediction interval	Nominal level, such as 0.95	Wide uncertainty at small counts (Figure 5)	Preprint[59]
Standardized residual RMS	Size of residuals relative to the predicted deviation	1	Needs measurement noise in the deviation	Preprint[60]
Regression calibration curve	Predicted quantile levels against observed frequencies	Identity line	Needs enough points per level	Peer-reviewed[61]
Conformal coverage	Finite-sample marginal coverage from a calibration set	Nominal or higher on average	Spread around the average at small sizes	Monograph and preprint[6263]
Noise-aware interval width	Width of the interval for noisy outputs	Root of predictive variance plus noise variance	Needs an estimate of measurement noise	Preprint[64]
Calibration under dataset shift	Change in calibration when inputs leave the training region	Coverage maintained in each region	Reported to degrade	Conference paper[6566]

The metrics are those in the cited sources. The limits column summarizes the sources and the calculations in this paper.

5.3 Scoring each hardware batch before training keeps the test independent of the model it checks

A batch of measurements has two uses, and the order decides whether they are independent. Scored against the current surrogate before training, the batch measures the model that engineers used. Added to the training set first, it measures a model that has seen the answer. The test-before-train order produces the coverage count, the standardized residuals and the share of points outside the training region for each batch, and it fits the data flywheel that SOL describes, in which coupon, single-jet and prototype data recalibrate the surrogate.[67] The provenance model of W3C records the entities, activities and agents behind each data set, and the NIST risk framework supplies functions for measuring and managing model risk.[6869] A credibility assessment in the style of ASME V&V 40 links the evidence to the context of use, and the context for CF-JET is the release of a design for printing.[70] The sources supply elements of a record, and no retrieved source prescribes the record for a surrogate of thermal hardware.

6. University Test and Fabrication Capacity in Alabama and Mississippi

6.1 Documented capacity covers printing and manufacturing training, and thermal-fluid testing and CT are documented only at Auburn

Table 12 lists what retrieved public sources document. Alabama A&M University documents a makerspace laboratory with a 3D printer, and a fiscal 2024 Department of Defense award of $595,401 for a thin-film deposition system, a laser marker and optical and chemical characterization systems.[7172] Tuskegee University documents a Chevron additive manufacturing laboratory and a NASA research and education award for additive manufacturing in aerospace, in which Tuskegee is the only HBCU among three recipients.[7374] Jackson State University lists a research laboratory with a 3D printer production system in its engineering building.[75] Calhoun Community College describes an additive manufacturing program with more than 4,000 square feet, polymer and metal post-processing labs for 16 students, and a statement

that it offers the only design additive manufacturing program in Alabama.[76] In Mississippi, the Gulf Coast and East Mississippi community colleges host Advancements in Manufacturing Upskilling Program labs developed with Mississippi State University, with collaborative robots, resin and metal 3D printers, 3D scanning, and an advanced composites training center, and Meridian Community College received a $1.1 million grant for metal 3D printing, coordinate measuring machine inspection and mechatronics.[777879]

Table 12. Documented capabilities relevant to CF-JET testing in Alabama and Mississippi

Institution	Documented capability	Relevance to the test ladder	Evidence
Auburn University	X-ray CT system acquired with a 2016 NIST grant, in a vault that accommodates additive manufacturing machines	Micro-CT of printed parts (Table 9)	University publication[80]
Alabama A&M University (HBCU)	Makerspace lab with 3D printer; fiscal 2024 DoD award for thin-film deposition, laser marker, optical and chemical characterization	Coupon fabrication; surface and coating characterization	Institutional news[8182]
Tuskegee University (HBCU)	Chevron additive manufacturing laboratory; NASA research and education award in additive manufacturing	Printing and aerospace additive manufacturing research	News and trade[8384]
Jackson State University (HBCU)	Research lab with 3D printer production system; robotics and electronics teaching labs	Printing; data-acquisition and controls skills	Institutional web page[85]
Calhoun Community College	Additive manufacturing program, more than 4,000 square feet, polymer and metal post-processing labs	Printing and post-processing of coupons	Institutional web page[86]
Mississippi Gulf Coast and East Mississippi community colleges	Manufacturing upskilling labs with resin and metal 3D printers, 3D scanning, collaborative robots, composites training center	Printing, scanning, composite layup training	Institutional news[8788]
Meridian Community College	Grant for metal 3D printing, coordinate measuring machine inspection, mechatronics	Dimensional inspection of printed plates	News report[89]

The table lists what retrieved sources state. No retrieved source documents a coolant flow loop, laser flash, thermomechanical analysis, thermal cycling or micro-CT at an HBCU or community college in either state, and no retrieved source covers Alcorn State, Mississippi Valley State, Alabama State, Stillman, Oakwood or Tougaloo.

The match between documented capacity and the test ladder in Figure 1 is partial. Coupon printing, post-processing, scanning and dimensional inspection have documented homes in both states. The ladder's thermal-fluid stages need a heater block, a pump, a flowmeter, heat exchangers, a data acquisition system and a controls layer, which is the equipment list of the university metrology rig.[90] The retrieved sources for Jackson State and the Mississippi community colleges describe robotics, automation and electronics labs, which cover the controls and data acquisition parts of that list. Whether those labs can build and operate a flow loop is a proposal for the CF-JET team to test with a scoping visit, and the retrieved sources do not show it. Alabama A&M University students already worked with SOL on the HVAC modeling that led to SOL Aquifer, which gives a documented relationship to build on.[91]

7. Implications for the CF-JET Effort

7.1 Risks

Table 13. Risks to hardware validation of the CF-JET surrogate

Risk	Basis	Mitigation	Evidence
Acceptance of 0.02 K/W falls inside rig uncertainty	Reported ±10.6 percent on 0.0198 K/W; instrument terms ±3.0 percent	Guard-banded limit; calibrate the rig with a reference plate; state the uncertainty with each result	Reported and computed[92]
Test definition differs between laboratories	Case-temperature definition changed resistance by 3.3 to 42.9 percent; joining pressure by 34.2 percent	Fix the case-temperature definition, interface material and joining pressure in the test plan	Peer-reviewed[93]
Through-thickness conductivity cannot be taken from a standard	E1461 and D5470 scopes do not address oriented inserts; contact resistance biased a single specimen low by 33 to 75 percent	Multi-thickness coupons with a controlled interface; lateral diffusion check	Standards and computed[9495]
Defects under 90 µm escape full-plate CT	A 30 µm voxel detects 90 µm features	Sub-region scans at 5 µm or finer; trial scan of plated coupons	Computed and reported[96]
Validation set too small to confirm coverage	46 points needed to separate 95 from 85 percent coverage	Report counts with intervals; pool batches by region; replicate measurements	Computed
Thermal-fluid and CT capacity at HBCUs and community colleges is undocumented	No retrieved source documents a flow loop, laser flash or CT there	Scoping visits; use Auburn for CT; build a single-jet rig as a teaching project	Evidence gap

The evidence column states whether the basis is reported in a source, computed for this paper or a gap in the retrieved literature.

7.2 Design implications

- **Write the test definition into the requirement.** The 0.02 K/W statement names the case-temperature definition, the interface material, the joining pressure and the inlet temperature. The surrogate takes the same quantities as inputs.
- **Add a guard band.** The acceptance limit equals the requirement less the expanded uncertainty, and the report states the uncertainty. At instrument-only level the limit is 0.0194 K/W, and at the university-rig level it is 0.0179 K/W (computed).
- **Match the temperature pair.** Heat-balance checks at 4 to 8 L/min need a matched inlet and outlet pair near ±0.05 K, since coolant rise is 3 to 6 K.
- **Perform resistance tests at the design inlet.** The reference temperature of 45 °C in the specification differs from the 65 °C inlet, so fluid properties and set point are recorded for each test.
- **Measure coupons at several thicknesses.** A regression on five thicknesses recovered conductivity where single-specimen readings gave 33 to 75 percent of the true value in the model (computed). Each coupon records interface material and contact pressure.
- **Choose CT voxel size from the feature of interest.** Full-plate scans at 30 µm find large voids, and 5 µm sub-region scans find the pore population. Thresholds are calibrated on a known specimen.
- **Score before training.** Each hardware batch is scored against the current surrogate with measurement noise added to the interval width, and the counts, coverage and standardized residuals enter the release record.

7.3 Open research questions

- What through-thickness conductivity do carbon fiber plates with perpendicular pitch fiber inserts have at several insert pitches, and which method gives the smallest uncertainty?
- Does laser flash on such plates show lateral diffusion that violates the one-dimensional model, and how large is the resulting bias?

- Can micro-CT detect voids and delamination in the electroplated coolant face and its bond to the body, and at what voxel size?
- What case-temperature definition and interface reproduce the CF-JET heat path in a thermal test vehicle with the smallest uncertainty?
- How many validation plates per region are needed to confirm 95 percent coverage when measurement noise is half the prediction deviation?
- Which HBCU or community college laboratories can build and operate a single-jet rig and a flow loop within the program schedule?

8. Conclusion

Hardware tests for the CF-JET plate fix the evidence that confirms or rejects surrogate predictions, and the quality of that evidence depends on the test definition. Instrument terms give ±3.0 percent on thermal resistance at 1.5 kW (computed), while published rig studies show 3.3 to 42.9 percent differences from the definition of case temperature and 34.2 percent from joining pressure. The standards that apply define procedure and state no accuracy, and no retrieved source measures through-thickness conductivity of a pitch-fiber-insert composite or the micro-CT detectability of an electroplated coolant face.

Three conditions decide whether a comparison of prediction intervals with hardware is valid. The test definition and its uncertainty are stated with each measurement and carried into the interval width. The validation set is large enough for the claim, which needs 46 points to separate 95 percent from 85 percent coverage in one region (computed). Each batch is scored before it joins the training set. Auburn documents the one CT system found, and the Alabama and Mississippi HBCUs and community colleges document printing, scanning and manufacturing training that fit the coupon and fabrication stages. Their capacity for the thermal-fluid stages is an open question for a scoping visit.

Bibliography

Alabama A&M University. “Alabama A&M Researchers Awarded $595,000 DoD Grant to Advance STEM Education and Renewable Energy Research.” News release, n.d. https://www.aamu.edu/about/inside-aamu/news/grant-will-fund-equipment-for-energy-harvesting-and-storage-research.html. Institutional news release.

Alabama A&M University. “AAMU Student Developed EpiPen Case in Bulldog Makerspace Lab.” News release, 23 April 2026. https://www.aamu.edu/about/inside-aamu/news/mubanga-developed-epipen-case-in-bulldog-makerspace-lab.html. Institutional news release.

Angelopoulos, Anastasios N., and Stephen Bates. “Conformal Prediction: A Gentle Introduction.” *Foundations and Trends in Machine Learning* 16, no. 4 (2023): 494–591. https://doi.org/10.1561/2200000101.

American Society of Mechanical Engineers. *Standard for Verification and Validation in Computational Fluid Dynamics and Heat Transfer*. ASME V&V 20-2009 (R2016). New York: ASME, 2009. https://webstore.ansi.org/Standards/ASME/ASME202009R2016.

American Society of Mechanical Engineers. “Bioengineering Blog: An Emerging Regulatory Framework for Medical Device Simulation.” ASME, n.d. https://www.asme.org/topics-resources/content/bioengineering-blog-an-emerging-regulatory-framework-for-medical-device-simulation. Publisher blog describing standard ASME V&V 40-2018; the standard itself was not read.

ASTM International. *ASTM D5470-17, Standard Test Method for Thermal Transmission Properties of Thermally Conductive Electrical Insulation Materials*. Catalog entry. https://store.astm.org/d5470-17.html. Cited by

designation and catalog text; standard text is not reproduced.

ASTM International. *ASTM E1461-13(2022), Standard Test Method for Thermal Diffusivity by the Flash Method*. Catalog entry. https://standards.iteh.ai/catalog/standards/astm/a51806df-fbd2-459c-b8b4-a23e5f2244b0/astm-e1461-13-2022. Cited by designation and catalog text; standard text is not reproduced.

ASTM International. *ASTM E1461-92, Standard Test Method for Thermal Diffusivity of Solids by the Flash Method*. Historical catalog entry. https://store.astm.org/e1461-92.html. Superseded edition, cited for its scope text; standard text is not reproduced.

ASTM International. *ASTM E831-25, Standard Test Method for Linear Thermal Expansion of Solid Materials by Thermomechanical Analysis*. Catalog entry. https://webstore.ansi.org/standards/astm/astme83125. Cited by designation and catalog text; standard text is not reproduced.

Auburn University Samuel Ginn College of Engineering. “The Game Changer.” 2019. https://eng.auburn.edu/asee/2019/auburn-nist-grant-psx-macro-ct. University publication.

Baillie, Nils, Baptiste Kerleguer, Cyril Feau, and Josselin Garnier. “Multi-Fidelity Gaussian Process Regression for Noisy Outputs and Non-Nested Experimental Designs: Decoupled versus Joint Likelihood Optimization.” arXiv:2511.20183. Preprint, 26 November 2025. https://arxiv.org/abs/2511.20183.

Calhoun Community College. “Alabama Center for Additive Manufacturing Excellence.” Web page, n.d. https://calhoun.edu/technologies/additive-manufacturing/. Institutional web page.

East Mississippi Community College. “EMCC, MSU Host Ribbon Cutting at The Communiversity to Highlight Partnership.” News release, 2025. https://www.eastms.edu/news/2025/emcc-msu-partnership-communiversity-2025.html. Institutional news release.

Guo, Chuan, Geoff Pleiss, Yu Sun, and Kilian Q. Weinberger. “On Calibration of Modern Neural Networks.” *Proceedings of the 34th International Conference on Machine Learning*, PMLR 70 (2017): 1321–1330. https://proceedings.mlr.press/v70/guo17a.html.

“Tuskegee 3-D Printing Laboratory.” HBCU Lifestyle, last updated 27 September 2019. https://hbculifestyle.com/tuskegee-3-d-printing-laboratory. Trade and news material.

Jackson State University, Department of Civil and Environmental Engineering and Industrial Systems and Technology. “Technology Department Facilities.” Web page, n.d. https://www.jsums.edu/industrialsystems/technology-department-facilities/. Institutional web page.

JEDEC Solid State Technology Association. *JESD22-A104F.01, Temperature Cycling*. April 2023. Catalog entry at https://standards.globalspec.com/std/14597601/jesd22-a104f-01.

Joshi, C. “Effects of Thermal Interface Materials on Thermal Conductivity Measurement Using a Modified ASTM D5470 Thermal Resistance Tester.” Mechanical Engineering Undergraduate Honors Theses, University of Arkansas, 2025. https://scholarworks.uark.edu/meeguht/140. Undergraduate honors thesis.

Kuleshov, Volodymyr, Nathan Fenner, and Stefano Ermon. “Accurate Uncertainties for Deep Learning Using Calibrated Regression.” *Proceedings of Machine Learning Research* 80 (2018): 2796–2804.

Martinez, Victor A., Carol Caceres, and Alfonso Ortega. “Development of a Thermal Metrology Standard for Evaluation of Cold Plate Thermal Resistance as a Performance Metric.” *Journal of Electronic Packaging* 146, no. 4 (2024): 041118. https://doi.org/10.1115/1.4066101.

“Mississippi College Board Awards $1.1 Million for Advanced Manufacturing Tech Program.” *Government Technology* (TNS), n.d. https://www.govtech.com/education/higher-ed/Mississippi-College-Board-Awards-11-Million-for-Advanced-Manufacturing-Tech-Program.html. News report.

Mississippi Gulf Coast Community College. “AiM UP Lab Grand Opening.” News release, n.d. https://mgccc.edu/?p=39800. Institutional news release.

National Institute of Standards and Technology. *Artificial Intelligence Risk Management Framework (AI RMF 1.0)*. NIST AI 100-1. Gaithersburg, MD: NIST, January 2023. https://doi.org/10.6028/NIST.AI.100-1.

Nokia Bell Labs. “A High-Precision Apparatus for the Characterization of Thermal Interface Materials.” Publication record, 1 September 2009. https://www.nokia.com/bell-labs/publications-and-media/publications/a-high-precision-apparatus-for-the-characterization-of-thermal-interface-materials/. Corporate research laboratory summary.

Oak Ridge National Laboratory. “Benchmarking Image Processing Techniques for Porosity Measurement in Polymer Additive Manufacturing: Review and Experimental Analysis.” *Composites Part B: Engineering* 307, article 112857. Publication record. https://www.ornl.gov/publication/benchmarking-image-processing-techniques-porosity-measurement-polymer-additive. Government laboratory publication record; authors not listed in the retrieved record.

Sutton, Ben, Brad Zakaib, Gerald Singer, Ian Winfield, and Tyler Loughran. *Single-Phase Direct-to-Chip Cold Plate Test Specification*. Version 1.0.0. Open Compute Project, 11 August 2026. https://www.opencompute.org/wp-content/uploads/2026/10/OCP-Cold-Plate-Test-Specification-V1.0.0.pdf. Industry specification; the primary author and one co-author are affiliated with a cold plate manufacturer.

Ortega, Alfonso, Victor A. Martinez, Carol Caceres, Ali Heydari, and Uschas Chowdhury. “Development of Thermal Metrology Standards for Experimental Characterization of Thermal Resistance for Single-Phase Liquid Cold Plates.” Paper IPACK2023-113883. *Proceedings of the ASME 2023 International Technical Conference and Exhibition on Packaging and Integration of Electronic and Photonic Microsystems*, San Diego, CA, 24–26 October 2023.

Ovadia, Yaniv, Emily Fertig, Jie Ren, Zachary Nado, D. Sculley, Sebastian Nowozin, Joshua V. Dillon, Balaji Lakshminarayanan, and Jasper Snoek. “Can You Trust Your Model’s Uncertainty? Evaluating Predictive Uncertainty under Dataset Shift.” *Advances in Neural Information Processing Systems* 32 (2019). arXiv:1906.02530. https://arxiv.org/abs/1906.02530.

Pelican Wire Company. “Thermocouple Tolerances.” Web page reproducing ASTM E230 limits of error, n.d. https://www.pelicanwire.com/thermocouple-wire/thermocouple-tolerances/. Trade (vendor) material.

Plank, Bernhard, Markus G. R. Sause, and Johann Kastner. “High-Resolution X-Ray Computed Tomography Simulations of Synthetically-Generated Volume Porosity in Continuous Carbon Fibre-Reinforced Polymer Samples.” *Nondestructive Testing and Evaluation* 37, no. 5 (2022): 645–665. https://doi.org/10.1080/10589759.2022.2086547.

Moreau, Luc, and Paolo Missier, eds. *PROV-DM: The PROV Data Model*. W3C Recommendation, 30 April 2013. https://www.w3.org/TR/2013/REC-prov-dm-20130430/.

Sánchez-Domínguez, Miguel, Lucas Lacasa, Javier de Vicente, Gonzalo Rubio, and Eusebio Valero. “Reliable Statistical Guarantees for Conformal Predictors with Small Datasets.” arXiv:2512.04566. Preprint, version 2, 16 December 2025. https://arxiv.org/abs/2512.04566.

Soete, Jeroen, Brice Badoux, Yentl Swolfs, Larissa Gorbatikh, and Martine Wevers. “Defect Detection in 3D Printed Carbon Fibre Composites Using X-Ray Computed Tomography.” Paper presented at the 9th Conference on Industrial Computed Tomography, Padova, Italy, 2019. https://lirias.kuleuven.be/retrieve/532962.

SOL Engineering Services, LLC. *CF-JET: AI/ML-Enabled Design and Development of an Additively Manufactured, Liquid-Cooled Jet-Impingement Cold Plate with Optimized Carbon Fiber Target Plate*. Proposal, Rev Final 2, n.d.

SOL Engineering Services, LLC. *SOL Aquifer* software pipeline diagram. n.d.

SOL Engineering Services, LLC. “Modeling HVAC System Performance: Code as Architecture Approach to AI.” Work carried out with Alabama A&M University students, n.d.

Tangsali, Kaustubh, Mohammad Amin Nabian, Kelvin Lee, Carmelo Gonzales, and Sanjay Choudhry. “Predictive Uncertainty for Neural CAE Surrogates.” arXiv:2609.25430. Preprint, 21 September 2026. https://arxiv.org/abs/2609.25430.

UNCF. “NASA Selects Tuskegee University to Help Advance Aerospace Manufacturing.” News item, n.d. https://uncf.org/?p=16977. Organization news item.

Notes

[1]Victor A. Martinez, Carol Caceres, and Alfonso Ortega, “Development of a Thermal Metrology Standard for Evaluation of Cold Plate Thermal Resistance as a Performance Metric,” *Journal of Electronic Packaging* 146, no. 4 (2024): 041118, https://doi.org/10.1115/1.4066101.

[2]Alfonso Ortega, Victor A. Martinez, Carol Caceres, Ali Heydari, and Uschas Chowdhury, “Development of Thermal Metrology Standards for Experimental Characterization of Thermal Resistance for Single-Phase Liquid Cold Plates,” paper IPACK2023-113883, *Proceedings of the ASME 2023 International Technical Conference and Exhibition on Packaging and Integration of Electronic and Photonic Microsystems* (San Diego, CA, 24–26 October 2023).

[3]Ben Sutton, Brad Zakaib, Gerald Singer, Ian Winfield, and Tyler Loughran, *Single-Phase Direct-to-Chip Cold Plate Test Specification*, Version 1.0.0 (Open Compute Project, 11 August 2026), https://www.opencompute.org/wp-content/uploads/2026/10/OCP-Cold-Plate-Test-Specification-V1.0.0.pdf.

[4]Martinez, Caceres, and Ortega, “Thermal Metrology Standard for Cold Plate Thermal Resistance.”

[5]ASTM International, *ASTM E1461-13(2022)*, *Standard Test Method for Thermal Diffusivity by the Flash Method*, catalog entry at https://standards.iteh.ai/catalog/standards/astm/a51806df-fbd2-459c-b8b4-a23e5f2244b0/astm-e1461-13-2022.

[6]ASTM International, *ASTM D5470-17*, *Standard Test Method for Thermal Transmission Properties of Thermally Conductive Electrical Insulation Materials*, catalog entry at https://store.astm.org/d5470-17.html.

[7]Jeroen Soete, Brice Badoux, Yentl Swolfs, Larissa Gorbatikh, and Martine Wevers, “Defect Detection in 3D Printed Carbon Fibre Composites Using X-Ray Computed Tomography,” paper presented at the 9th Conference on Industrial Computed Tomography (Padova, Italy, 2019), https://lirias.kuleuven.be/retrieve/532962.

[8]Bernhard Plank, Markus G. R. Sause, and Johann Kastner, “High-Resolution X-Ray Computed Tomography Simulations of Synthetically-Generated Volume Porosity in Continuous Carbon Fibre-Reinforced Polymer Samples,” *Nondestructive Testing and Evaluation* 37, no. 5 (2022): 645–665, https://doi.org/10.1080/10589759.2022.2086547.

[9]SOL Engineering Services, LLC, *CF-JET: AI/ML-Enabled Design and Development of an Additively Manufactured, Liquid-Cooled Jet-Impingement Cold Plate with Optimized Carbon Fiber Target Plate*, proposal, Rev Final 2, n.d.

[10]SOL Engineering Services, LLC, *SOL Aquifer* software pipeline diagram, n.d.

[11]SOL Engineering Services, LLC, “Modeling HVAC System Performance: Code as Architecture Approach to AI,” work carried out with Alabama A&M University students, n.d.

[12]Sutton et al., *Cold Plate Test Specification*.

[13]Sutton et al., *Cold Plate Test Specification*.

[14]Sutton et al., *Cold Plate Test Specification*.

[15]Sutton et al., *Cold Plate Test Specification*.

[16]Sutton et al., *Cold Plate Test Specification*.

[17]Sutton et al., *Cold Plate Test Specification*.

[18]Sutton et al., *Cold Plate Test Specification*.

[19]Sutton et al., *Cold Plate Test Specification*.

[20]Sutton et al., *Cold Plate Test Specification*.

[21]Martinez, Caceres, and Ortega, “Thermal Metrology Standard for Cold Plate Thermal Resistance.”

[22]Ortega et al., “Thermal Metrology Standards for Single-Phase Liquid Cold Plates.”

[23]Martinez, Caceres, and Ortega, “Thermal Metrology Standard for Cold Plate Thermal Resistance.”

[24]Ortega et al., “Thermal Metrology Standards for Single-Phase Liquid Cold Plates.”

[25]Martinez, Caceres, and Ortega, “Thermal Metrology Standard for Cold Plate Thermal Resistance.”

[26]Ortega et al., “Thermal Metrology Standards for Single-Phase Liquid Cold Plates.”

[27]Pelican Wire Company, “Thermocouple Tolerances,” web page reproducing ASTM E230 limits of error, n.d., https://www.pelicanwire.com/thermocouple-wire/thermocouple-tolerances/.

[28]Pelican Wire, “Thermocouple Tolerances.”

[29]Pelican Wire, “Thermocouple Tolerances.”

[30]Martinez, Caceres, and Ortega, “Thermal Metrology Standard for Cold Plate Thermal Resistance.”

[31]Ortega et al., “Thermal Metrology Standards for Single-Phase Liquid Cold Plates.”

[32]Nokia Bell Labs, “A High-Precision Apparatus for the Characterization of Thermal Interface Materials,” publication record, 1 September 2009, https://www.nokia.com/bell-labs/publications-and-media/publications/a-high-precision-apparatus-for-the-characterization-of-thermal-interface-materials/.

[33]Sutton et al., *Cold Plate Test Specification*.

[34]ASTM E1461-13(2022).

[35]ASTM International, *ASTM E1461-92, Standard Test Method for Thermal Diffusivity of Solids by the Flash Method*, historical catalog entry at https://store.astm.org/e1461-92.html.

[36]ASTM D5470-17.

[37]Nokia Bell Labs, “High-Precision Apparatus for Thermal Interface Materials.”

[38]C. Joshi, “Effects of Thermal Interface Materials on Thermal Conductivity Measurement Using a Modified ASTM D5470 Thermal Resistance Tester,” Mechanical Engineering Undergraduate Honors Theses (University of Arkansas, 2025), https://scholarworks.uark.edu/meeguht/140.

[39]ASTM E1461-13(2022).

[40]ASTM D5470-17.

[41]Joshi, “Modified ASTM D5470 Thermal Resistance Tester.”

[42]Nokia Bell Labs, “High-Precision Apparatus for Thermal Interface Materials.”

[43]ASTM International, *ASTM E831-25, Standard Test Method for Linear Thermal Expansion of Solid Materials by Thermomechanical Analysis*, catalog entry at https://webstore.ansi.org/standards/astm/astme83125.

[44]JEDEC Solid State Technology Association, *JESD22-A104F.01, Temperature Cycling*, April 2023, catalog entry at https://standards.globalspec.com/std/14597601/jesd22-a104f-01.

[45]Soete et al., “Defect Detection in 3D Printed Carbon Fibre Composites.”

[46]Soete et al., “Defect Detection in 3D Printed Carbon Fibre Composites.”

[47]Plank, Sause, and Kastner, “X-Ray Computed Tomography Simulations of Synthetic Porosity.”

[48]Plank, Sause, and Kastner, “X-Ray Computed Tomography Simulations of Synthetic Porosity.”

[49]Oak Ridge National Laboratory, “Benchmarking Image Processing Techniques for Porosity Measurement in Polymer Additive Manufacturing: Review and Experimental Analysis,” *Composites Part B: Engineering* 307, article 112857, publication record, https://www.ornl.gov/publication/benchmarking-image-processing-techniques-porosity-measurement-polymer-additive.

[50]Soete et al., “Defect Detection in 3D Printed Carbon Fibre Composites.”

[51]Plank, Sause, and Kastner, “X-Ray Computed Tomography Simulations of Synthetic Porosity.”

[52]Auburn University Samuel Ginn College of Engineering, “The Game Changer,” 2019, https://eng.auburn.edu/asee/2019/auburn-nist-grant-psx-macro-ct.

[53]Nils Baillie, Baptiste Kerleguer, Cyril Feau, and Josselin Garnier, “Multi-Fidelity Gaussian Process Regression for Noisy Outputs and Non-Nested Experimental Designs: Decoupled versus Joint Likelihood Optimization,” arXiv:2511.20183 (preprint, 26 November 2025), https://arxiv.org/abs/2511.20183.

[54]American Society of Mechanical Engineers, *Standard for Verification and Validation in Computational Fluid Dynamics and Heat Transfer*, ASME V&V 20-2009 (R2016) (New York: ASME, 2009), https://webstore.ansi.org/Standards/ASME/ASME202009R2016.

[55]Anastasios N. Angelopoulos and Stephen Bates, “Conformal Prediction: A Gentle Introduction,” *Foundations and Trends in Machine Learning* 16, no. 4 (2023): 494–591, https://doi.org/10.1561/2200000101.

[56]Miguel Sánchez-Domínguez, Lucas Lacasa, Javier de Vicente, Gonzalo Rubio, and Eusebio Valero, “Reliable Statistical Guarantees for Conformal Predictors with Small Datasets,” arXiv:2512.04566 (preprint, version 2, 16 December 2025), https://arxiv.org/abs/2512.04566.

[57]Kaustubh Tangsali, Mohammad Amin Nabian, Kelvin Lee, Carmelo Gonzales, and Sanjay Choudhry, “Predictive Uncertainty for Neural CAE Surrogates,” arXiv:2609.25430 (preprint, 21 September 2026), https://arxiv.org/abs/2609.25430.

[58]Yaniv Ovadia et al., “Can You Trust Your Model’s Uncertainty? Evaluating Predictive Uncertainty under Dataset Shift,” *Advances in Neural Information Processing Systems* 32 (2019), arXiv:1906.02530, https://arxiv.org/abs/1906.02530.

[59]Tangsali et al., “Predictive Uncertainty for Neural CAE Surrogates.”

[60]Tangsali et al., “Predictive Uncertainty for Neural CAE Surrogates.”

[61]Volodymyr Kuleshov, Nathan Fenner, and Stefano Ermon, “Accurate Uncertainties for Deep Learning Using Calibrated Regression,” *Proceedings of Machine Learning Research* 80 (2018): 2796–2804.

[62]Angelopoulos and Bates, “Conformal Prediction.”

[63]Sánchez-Domínguez et al., “Conformal Predictors with Small Datasets.”

[64]Baillie et al., “Multi-Fidelity Gaussian Process Regression for Noisy Outputs.”

[65]Ovadia et al., “Can You Trust Your Model’s Uncertainty?”

[66]Chuan Guo, Geoff Pleiss, Yu Sun, and Kilian Q. Weinberger, “On Calibration of Modern Neural Networks,” *Proceedings of the 34th International Conference on Machine Learning*, PMLR 70 (2017): 1321–1330, https://proceedings.mlr.press/v70/guo17a.html.

[67]SOL Engineering Services, *CF-JET*, Rev Final 2.

[68]Luc Moreau and Paolo Missier, eds., *PROV-DM: The PROV Data Model*, W3C Recommendation (30 April 2013), https://www.w3.org/TR/2013/REC-prov-dm-20130430/.

[69]National Institute of Standards and Technology, *Artificial Intelligence Risk Management Framework (AI RMF 1.0)*, NIST AI 100-1 (Gaithersburg, MD: NIST, January 2023), https://doi.org/10.6028/NIST.AI.100-1.

[70]American Society of Mechanical Engineers, “Bioengineering Blog: An Emerging Regulatory Framework for Medical Device Simulation,” ASME, n.d., https://www.asme.org/topics-resources/content/bioengineering-blog-an-emerging-regulatory-framework-for-medical-device-simulation.

[71]Alabama A&M University, “AAMU Student Developed EpiPen Case in Bulldog Makerspace Lab,” news release, 23 April 2026, https://www.aamu.edu/about/inside-aamu/news/mubanga-developed-epipen-case-in-bulldog-makerspace-lab.html.

[72]Alabama A&M University, “Alabama A&M Researchers Awarded $595,000 DoD Grant to Advance STEM Education and Renewable Energy Research,” news release, n.d., https://www.aamu.edu/about/inside-aamu/news/grant-will-fund-equipment-for-energy-harvesting-and-storage-research.html.

[73]“Tuskegee 3-D Printing Laboratory,” HBCU Lifestyle, last updated 27 September 2019, https://hbculifestyle.com/tuskegee-3-d-printing-laboratory.

[74]UNCF, “NASA Selects Tuskegee University to Help Advance Aerospace Manufacturing,” news item, n.d., https://uncf.org/?p=16977.

[75]Jackson State University, Department of Civil and Environmental Engineering and Industrial Systems and Technology, “Technology Department Facilities,” web page, n.d., https://www.jsums.edu/industrialsystems/technology-department-facilities/.

[76]Calhoun Community College, “Alabama Center for Additive Manufacturing Excellence,” web page, n.d., https://calhoun.edu/technologies/additive-manufacturing/.

[77]Mississippi Gulf Coast Community College, “AiM UP Lab Grand Opening,” news release, n.d., https://mgccc.edu/?p=39800.

[78]East Mississippi Community College, “EMCC, MSU Host Ribbon Cutting at The Communiversity to Highlight Partnership,” news release, 2025, https://www.eastms.edu/news/2025/emcc-msu-partnership-communiversity-2025.html.

[79]“Mississippi College Board Awards $1.1 Million for Advanced Manufacturing Tech Program,” *Government Technology* (TNS), n.d., https://www.govtech.com/education/higher-ed/Mississippi-College-Board-Awards-11-Million-for-Advanced-Manufacturing-Tech-Program.html.

[80]Auburn University, “The Game Changer.”

[81]Alabama A&M University, “Bulldog Makerspace Lab.”

[82]Alabama A&M University, “$595,000 DoD Grant.”

[83]“Tuskegee 3-D Printing Laboratory.”

[84]UNCF, “NASA Selects Tuskegee University.”

[85]Jackson State University, “Technology Department Facilities.”

[86]Calhoun Community College, “Additive Manufacturing Excellence.”

[87]Mississippi Gulf Coast Community College, “AiM UP Lab.”

[88]East Mississippi Community College, “Communiversity Partnership.”

[89]“Mississippi College Board Awards $1.1 Million.”

[90]Ortega et al., “Thermal Metrology Standards for Single-Phase Liquid Cold Plates.”

[91]SOL Engineering Services, “Modeling HVAC System Performance.”

[92]Ortega et al., “Thermal Metrology Standards for Single-Phase Liquid Cold Plates.”

[93]Martinez, Caceres, and Ortega, “Thermal Metrology Standard for Cold Plate Thermal Resistance.”

[94]ASTM E1461-13(2022).

[95]ASTM D5470-17.

[96]Soete et al., “Defect Detection in 3D Printed Carbon Fibre Composites.”